Toward a Traceless Tag for the Thiol-Mediated Uptake of Proteins

Maynard, John; Saidjalolov, Saidbakhrom; Velluz, Marie-Claire; Vossio, Stefania; Aumeier, Charlotte; Moreau, Dimitri; Sakai, Naomi; Matile, Stefan

ChemistryEurope
Excellence in Chemistry Research Worldwide

Research Article
doi.org/10.1002/ceur.202300029

www.journal.chemistry-europe.org

Toward a Traceless Tag for the Thiol-Mediated Uptake of Proteins

John R. J. Maynard,[a] Saidbakhrom Saidjalolov,[a] Marie-Claire Velluz,[b] Stefania Vossio,[c] Charlotte Aumeier,[b] Dimitri Moreau,[c] Naomi Sakai,[a] and Stefan Matile*[a]

The emergence of thiol-mediated uptake (TMU) as a powerful strategy to penetrate cells calls for the development of practical small-molecule TMU tools for traceless delivery. Toward this goal, esters are explored here as bioreversible linkers between dynamic covalent cascade exchangers accounting for TMU and the protein of interest (POI). The method relies on α-aryl-α-diazoamides that react with carboxylic acids of the POI to form esters that can be enzymatically hydrolyzed inside cells to release the native POI. A two-step protocol is established for bioreversible conjugation of TMU tags to the POI. Despite the small number of tags attached to POIs to prevent isoelectric precipitation, POIs with traceless TMU tags are shown to efficiently enter cells not only in 2D culture but also in 3D spheroids mimicking deep tissue, confirming a key advantage of TMU. Uptake inhibition by various thiol-reactive agents confirms the participation of cell-surface thiols in cell penetration, i.e., the occurrence of TMU.

Introduction

Cell penetration is a persistent challenge of utmost importance in science and society: It is where most drugs fail and the worst pathogens excel. Among several known pathways to reach the cytosol, direct translocation across the plasma membrane is the most straightforward and desirable to avoid endo-lysosomal capture and degradation. So far, most studies on direct translocation have focused on cell-penetrating peptides (CPPs),[1–6] which are effective but have intrinsic limitations including somewhat unpredictable toxicity, a tendency toward endocytosis with increasing substrate size, resulting in endosomal capture, and an overall poor ability to penetrate deep tissue.

In recent years, thiol-mediated uptake (TMU) has been increasingly recognized as an alternative pathway to enter cells directly.[7–11] TMU stands for the emergence of cell-penetrating capacity in substrates upon the attachment of thiol-reactive agents, such as reversible cascade exchangers or CAXs. CAXs are dynamic covalent chemistry motifs that can exchange multiple times with cellular thiol/ates and disulfides without losing covalent contact. TMU is revealed by its competitive inhibition with thiol-reactive agents, including the same CAXs (Figure 1a).[7] The best explored CAXs are disulfides, in particular, strained cyclic disulfides such as the most popular asparagusic acid (AspA). Since the introduction of cell-penetrating polydisulfides,[12] followed by AspA for TMU with small molecules,[13] a variety of CAXs has been shown to deliver diverse substrates into various targets.[7] This includes the delivery of genome editing machinery,[14] various forms of genes,[15–19] phosphorothioate oligonucleotides,[20] antibodies[8] and other proteins,[21–24] and nanoparticles,[8,25–29] to living animals,[14] plant cells,[18] bacteria,[30] and into deep tissue.[24] Inhibition of TMU has been linked to drug discovery with regard to antiviral, antithrombotic and antitumor potential.[30–36] Only the transferrin receptor[37] and the integrin superfamily[31] have been identified so far as exchange partners in the complex networks that presumably enable TMU. The challenging nature of the dynamic covalent cascade exchange chemistry operating these networks is presumably the reason why TMU is not better known, understood and used.[7]

The proven power of TMU for cell penetration calls for general TMU tools to solve practical delivery problems in a simple and reliable manner. While various TMU methods for oligonucleotide delivery are rapidly evolving,[14–19,38] traceless small-molecule tags accessible for the broader community to easily and reliably deliver proteins of interest (POIs) do not exist. Such ideal small-molecule TMU tags could be attached to the POI *in situ* under bioorthogonal conditions prior to delivery and detached after uptake in the cytosol to release the POI in its native form (Figure 1c). Many elegant bioconjugation strategies are available to react with protein surface lysines, glutamates, aspartates, cysteines, methionines, tyrosines and arginines.[39–58]

[a] *Dr. J. R. J. Maynard, Dr. S. Saidjalolov, Dr. N. Sakai, Prof. S. Matile*
Department of Organic Chemistry
University of Geneva
1211 Geneva (Switzerland)
E-mail: stefan.matile@unige.ch
Homepage: www.unige.ch/sciences/chiorg/matile/

[b] *M.-C. Velluz, Prof. C. Aumeier*
Department of Biochemistry
University of Geneva
1211 Geneva (Switzerland)

[c] *S. Vossio, Dr. D. Moreau*
ACCESS Geneva
University of Geneva
1211 Geneva (Switzerland)

Supporting information for this article is available on the WWW under https://doi.org/10.1002/ceur.202300029

Research Article
doi.org/10.1002/ceur.202300029

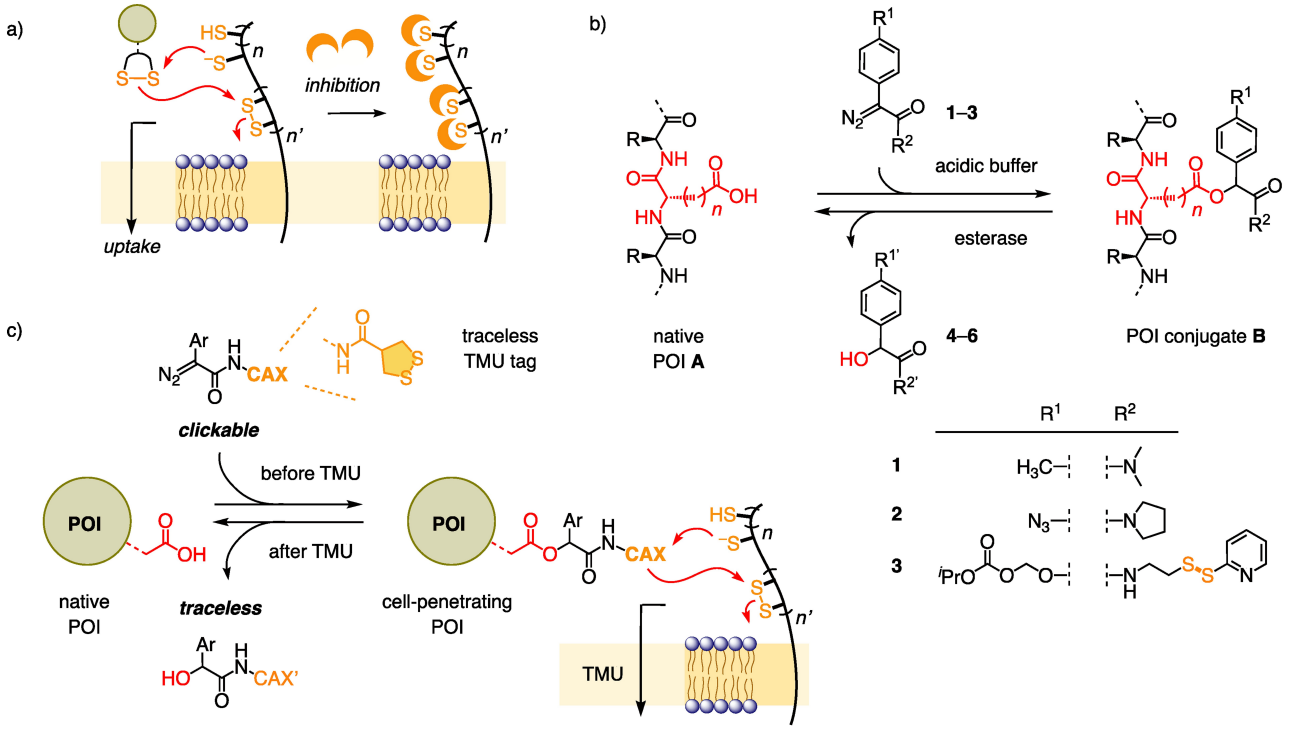

Figure 1. (a) Thiol-mediated uptake (TMU): Schematic representation of CAX-derivatized substrates engaging in dynamic covalent exchange cascades with cysteine thiolates/disulfides of membrane-associated proteins to penetrate cells, and characteristic inhibition with thiol-reactive compounds. (b) The bioreversible esterification of Glu ($n=2$) and Asp ($n=1$) residues in proteins of interest (POIs) by α-aryl-α-diazoamides under acidic conditions introduced by Raines and coworkers. c) The concept of traceless TMU tags based on bioreversible esterification, formulated with the intention to ultimately make TMU accessible to routinely solve delivery problems in practice. With AspA (an asparagusic-acid derivative) as representative CAX (cascade exchanger), which reversibly exchanges with cellular thiols to give CAX'.

Similarly diverse strategies have been reported as well to release the attached motifs in the cytosol.[39–47]

For the first attempt toward a clickable TMU tool for traceless delivery in practice, we selected a bioreversible esterification method that has been introduced by Raines and coworkers (Figure 1b).[39–42] In this method, the carboxylic acids of glutamate and aspartate residues in POI **A** react with α-aryl-α-diazoamides such as **1**–**3** to generate POI conjugate **B**. Ester hydrolysis catalyzed by cytosolic esterases would then reconvert POI conjugate **B** back to the native POI **A**, releasing the respective alcohols **4**–**6** as side products.

Bioreversible esterification reduces the number of negative charges and increases the hydrophobicity of the POI conjugate **B**, both of which are generally understood to be important factors in tuning affinity for the cell membrane. Early studies have shown that α-diazoamide **1** enabled the delivery of GFP and RNase A in cancer cells, where ester cleavage revealed the native proteins (Figure 1c).[40] Whilst this manuscript was in preparation, Raines and coworkers have further extended this strategy by modifying α-diazoamide tags in **2** and **3**[39,42] to enable the faster release of POIs, and the late-stage labeling of esterified proteins with a thiolated substrate, including CPPs[1–6] for promoting cellular uptake. In this study, we explore the potential of combining the Raines esterification approach and TMU for traceless protein delivery (Figure 1).

Results and Discussion

Functionalization of POIs with traceless TMU tags

The synthesis of traceless TMU tags based on bioreversible esterification required the combination of two functional motifs (Figure 1c). After numerous unsuccessful attempts to prepare a CAX containing α-aryl-α-diazoamides, we opted instead to apply a two-step functionalization approach as used previously for the preparation of cell-penetrating streptavidins.[57,58] In these studies, POIs were first decorated with the azide functionalities on lysine amines or tyrosine phenols, and then reacted with alkynylated CAXs by the copper-catalyzed azide-alkyne cycloaddition (CuAAC) reaction to achieve the CAX conjugation.[57,58] Replacement of the first irreversible bioconjugation step in this protocol by bioreversible esterification using azide-functionalized α-aryl-α-diazoamides should result in the desired, reversibly modified POIs with cell-penetrating capabilities.

The azide-functionalized α-aryl-α-diazoamide **7** was prepared following an improved synthesis developed by Raines and coworkers (Figure 2, Scheme S1).[41] GFP **8** was selected as the initial model POI. It soon became apparent that esterification under the original conditions gave low yields[59] of conjugate **9**, mainly due to the poor solubility of the product. This outcome could be attributed to the hydrophobic nature of

Research Article
doi.org/10.1002/ceur.202300029

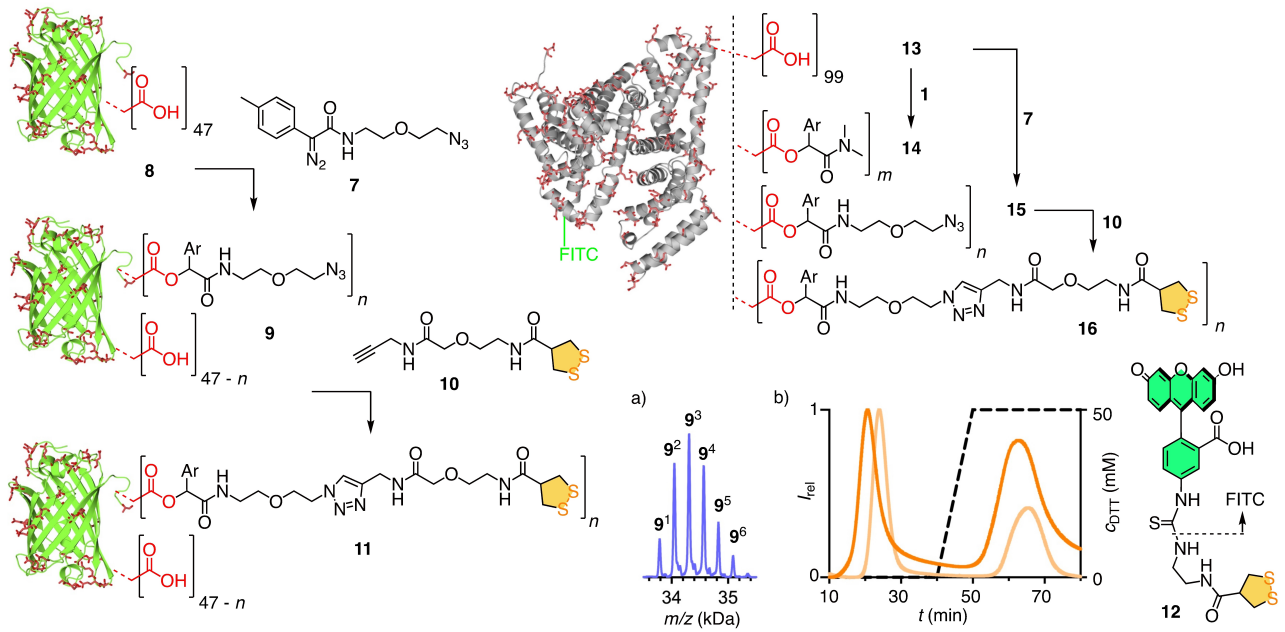

Figure 2. Derivatization of model POIs, affinity tagged GFP **8** and FITC-BSA **13**, with α-diazoamides **1** or **7** followed by CuAAC with alkyne **10**. (a) Deconvoluted ESI MS of esterified GFP **9**, and (b) elution profiles for samples of the TMU-tagged GFP **11** (dark orange) and AspA-FITC **12** (peach) passed through a thiol-affinity column, with 10 minute gradient of DTT from 0 to 50 mM after 40 min. Glu/Asp side chains of GFP and BSA are marked in red.

the ester and the removal of the negative charges resulting in an increasing isoelectric point toward isoelectric precipitation under physiological conditions.[60–62]

The appearance of isoelectric precipitation suggested that the number of esters should be kept low to preserve minimal solubility. Reaction conditions were therefore modified to improve yields whilst maintaining complete consumption of unfunctionalized GFP. Equivalents of α-diazoamide **7** could be reduced from 200 to 25, organic co-solvent modified from 20% MeCN to 2.5% DMSO, and NaCl (150 mM) was added to improve the solubility of the conjugate. Under optimized conditions, the most abundant species in ESI and MALDI MS characterization were $\mathbf{9}^3$ bearing 3 esters per protein (Figures 2a, S2). CuAAC of the azide decorated GFP **9** with AspA alkyne **10**, a readily accessible CAX repeatedly used in protein delivery applications, gave the GFP-CAX **11** for traceless TMU. The same strategy was also applied to generate the GFP conjugates with other CAXs including benzopolysulfanes, which were most active in cell-penetrating streptavidins.[57] However, they were not further followed up because of their apparent toxicity in initial uptake studies.

The reactivity of GFP-CAX **11** towards thiols was demonstrated by thiol-affinity chromatography (Figure 2b). GFP, lacking in native disulfide bonds, was partially retained by the thiolated stationary phase through covalent disulfide linkages to the appended CAXs until the addition of DTT reductant to the column eluent. The elution profile of the TMU-tagged POI **11** was similar to that of the previously reported[13] FITC-labeled AspA **12**.

To compare our two-step labeling approach against the delivery of proteins by esterification with α-diazoamide **1**, we selected fluorescein isothiocyanate labeled bovine serum albumin, FITC-BSA **13**, as a more soluble POI (Figure 2). With a larger number of carboxylic acids available, esterification of BSA-FITC was performed with 100 equivalents of α-diazoamides **1** or **7** under otherwise identical conditions as for GFP. In keeping with previous studies by Raines and coworkers,[39–41] the tertiary amide **1** proved to be a more efficient label than the secondary amide **7**, giving a higher degree of labeling in **14** ($m \approx 30$) compared to **15** ($n \approx 10$). CuAAC of the azide-rich BSA **15** with alkyne **10** provided desired TMU-tagged BSA **16**.

Delivery of GFP with traceless TMU tags

To quantify the separate impacts of esterification and attachment of CAX on protein delivery, the cellular uptake of GFP conjugates **9** and **11** was compared in HeLa-MZ cells by automated high-content high-throughput (AHCHT) microscopy at multiple concentrations following a 4 h incubation.[31,36,63] In initial experiments, cells were imaged both live and after fixation with 3% PFA, without notable differences in intensity or localization of fluorescent signals. However, as fixation reduced the background signal and removed some fluorescent aggregates which interfered with automated image analysis, subsequent analyses were conducted following PFA fixation (Figure S4).

The thiol-reactive GFP **11** showed uniform staining indicative of cytosolic delivery, with a higher intensity across all concentrations tested than esterified GFP control **9** (Figures 3a–c). The lack of staining with propidium iodide indicated that cell viability was maintained even at high concentrations of the

Research Article
doi.org/10.1002/ceur.202300029

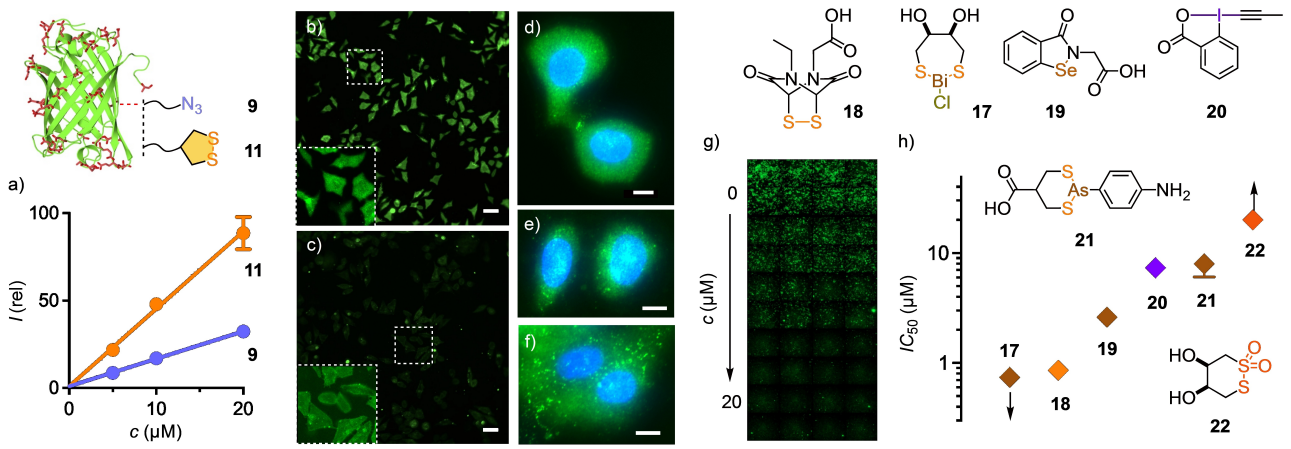

Figure 3. (a) Quantified cellular fluorescence for HeLa-MZ cells treated with the TMU-tagged GFP **11** (orange) and TMU-free GFP **9** (purple), following fixation. (b,c) Representative widefield images of HeLa-MZ cells after incubation with 10 μM of (b) TMU-tagged GFP **11**, or (c) TMU-free **9**. Scale bars = 50 μm. The imaging parameters were identical for b) and c), the brightness of the inset in c) was increased for better visibility. (d–f) Representative images of d) A431, e) MCF7, and f) h-RPE-1 cells after incubation with TMU-tagged GFP **11** (10 μM, green; blue, Hoechst 33342). Scale bars = 10 μm. (g) Representative fluorescence images of thousands of HeLa Kyoto cells incubated with a fixed concentration of TMU-tagged GFP **11** (4.5 μM) and a variable concentration of TMU inhibitor **18** to determine the IC_{50}. (h) IC_{50} of TMU probes **17**–**22** to inhibit cell penetration by the TMU-tagged GFP **11**.

conjugate (Figure S5). At higher concentrations of the TMU-tagged GFP **11**, strong staining of the cell was also noted at shorter incubation times (Figure S6). Moreover, uptake of the TMU-tagged GFP **11** was also demonstrated in A431, MCF-7, and h-RPE-1 cells, with dominant uniform staining seen in all cases (Figure 3d–f).

Inhibitors of TMU have been applied to prove the participation of cell-surface thiols in the delivery of substrates functionalized with thiol-reactive transporters. Whilst initial studies relied on a limited and less convincing pool of thiol-reactive reagents as inhibitors (iodoacetamide, DTNB), recent years have seen the development and application of chemically diverse libraries of thiol-reactive inhibitors as more sophisticated tools to explore protein networks participating in TMU pathways.[20,31–36,63]

With this in mind, we screened a small but chemically diverse selection of TMU inhibitors, i.e., **17**–**22**, against the TMU-tagged GFP **11**. The reduced GFP uptake was quantified by AHCHT microscopy in HeLa Kyoto cells to assure identical conditions with previous inhibitor screens, while the better quality images accessible with the otherwise very similar HeLa-MZ cells were not needed for AHCHT inhibitor screening (Figure 3g,h). Of these, the bismuth-centered exchanger **17** proved the most efficient,[33] followed by the strained cyclic disulfide **18**, an epidithiodiketopiperazine (ETP).[64] The submicromolar IC_{50} values were among the best ever observed for TMU, although the absolute values depend on the conditions used. The ebselen analog **19**, the hypervalent iodine reagent **20** and the arsenic-centered exchanger **21**[33] proved to be of middling efficiency. Finally, weak but significant inhibition was observed with cyclic thiosulfonate **22**[34] (for comparison, DTNB: MIC = 0.5 mM, IC_{50} not detectable[32]). These meaningful trends[32] from TMU inhibitors demonstrated that bioreversible esterification provides access to clickable TMU tools for the traceless delivery of POIs, here GFP.

Delivery of BSA with traceless TMU tags

The uptake of the three BSA conjugates **14**–**16** into HeLa-MZ cells was similarly examined. With the more hydrophobic and less negatively charged BSA **14**, fluorescence intensity within the cells was very weak and mostly contained within punctate structures (Figure 4a). This result was consistent with the known uptake pathway of albumins by receptor-mediated endocytosis.[65,66] Thus, fluorescence within cells but outside of puncta was quantified by applying masks to reveal negligible cytosolic delivery of **14** (Figure 4d). For TMU-free BSA **15**, a similar distribution of fluorescent signals was observed, although with greater intensity outside of puncta (Figure 4b,d). The TMU-tagged BSA **16** showed more intense and uniform

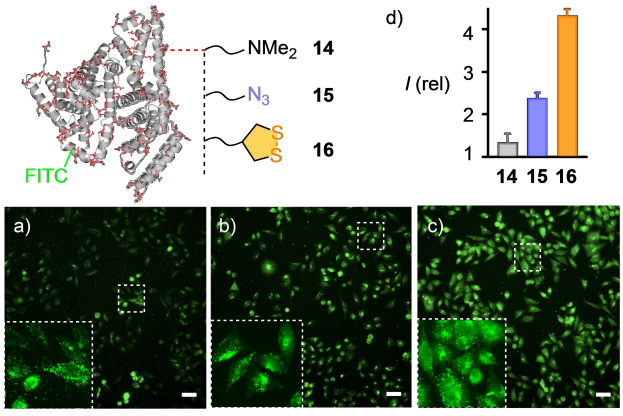

Figure 4. (a–c) Representative widefield images of HeLa-MZ cells incubated with (a) TMU-free **14** ($n \approx 30$), (b) TMU-free **15** ($n \approx 10$) and (c) the TMU-tagged BSA **16** ($n \approx 10$) under identical conditions. Scale bars = 50 μm. (d) Fluorescence intensity of HeLa-MZ cells after incubation with 2.5 μM **14**–**16** for 2 h. Fluorescence intensity is recorded only outside automatically masked puncta, usually indicative for endosomal capture, and normalized to blank fluorescence ($I = 1$).

Research Article
doi.org/10.1002/ceur.202300029

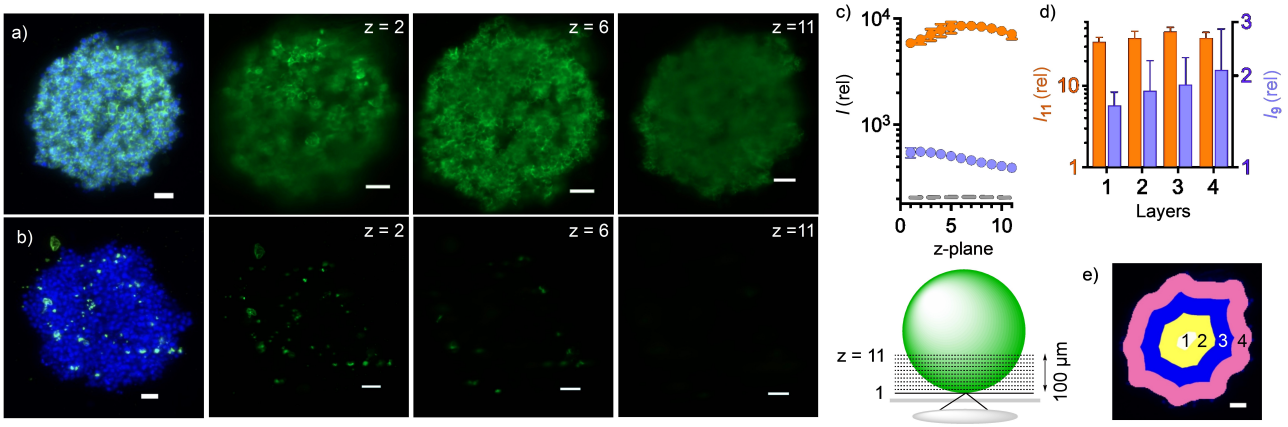

Figure 5. (a,b) Overlayed maximum projections of the green channel for GFP and the blue channel for cell nuclei (Hoechst 33342, left) and representative fluorescence images at three z-planes (10 μm separation per plane) of HeLa-MZ spheroids treated with (a) TMU-tagged GFP **11**, or (b) TMU-free GFP **9**. Scale bars = 50 μm. (c) Fluorescence intensities at different z-planes in HeLa-MZ spheroids (schematic drawing below) treated with TMU-free GFP **9** (purple), the TMU-tagged GFP **11** (orange), and none (grey). (d) Fluorescence enhancements relative to blank ($I = 1$) at different layers of spheroids treated with TMU-free **9** (purple) and the TMU-tagged GFP **11** (orange). (e) Representative layer (z = 6) mask for the spheroid in a).

staining of the cells with additional minor signals from punctate structures (Figure 4c,d). These results highlighted the power of TMU to deliver proteins to the cytosol against kinetic competition from endocytic processes.

Delivery into spheroids with traceless TMU tags

Efficient cytosolic delivery in deep tissue has been identified as a unique advantage of TMU, particularly when compared to standard CPPs.[24] The power of TMU to penetrate deep tissue has been explained with the transferrin receptors as one of the rare confirmed exchange partners in TMU.[24] Transferrin receptors are known for efficient transcytosis, important also to cross the blood-brain barrier and deliver iron to the brain. An expected dual function of transferrin receptor combining transcytosis with cell penetration by TMU provided thus a convincing explanation of the unique capacity of TMU to deliver into deep tissue.

To assess the capacity of the TMU-tagged GFP **11** for traceless delivery into deep tissue, HeLa-MZ cell spheroids with a diameter of around 350 μm were prepared as 3D tissue models (see Supporting Information for detailed experimental protocol).[24] After incubation with the TMU-tagged GFP **11**, spheroids were imaged both live and fixed to ensure fluorescent signal localization did not change. As in 2D culture, background signals were reduced following fixation. In 3D culture, the differences between the TMU-free GFP **9** and the TMU-tagged GFP **11** were even more marked than in 2D culture. Not only did the TMU-tagged GFP **11** yield a much greater net fluorescence intensity than TMU-free GFP **9** across a z-series of images through the spherical structure, but fluorescence intensity also peaked deeper into the spheroids (Figure 5a–c). With the TMU-tagged GFP **11**, fluorescence intensity at a depth of 60 μm (z = 6) from the spheroid surface is evenly distributed, whereas with the TMU-free GFP **9**, what little fluorescence intensity is present is localized to the outer layers of cells (Figure 5d,e). Decreasing laser penetration could contribute to weakened emission from the center of the spheroids, although more constant emission from Hoechst 33342 did not support this possibility. In any case, what really mattered were the much larger differences between TMU-tagged GFP **11** (Figure 5a) and TMU-free GFP **9** (Figure 5b), which also excluded spheroid penetration mechanisms other than thiol-mediated uptake. These results demonstrated that the unique power of TMU to deliver into deep tissue is preserved in clickable TMU tools for the traceless cytosolic delivery of POIs based on bioreversible esterification.

Conclusions

Toward a generally applicable TMU tool for the traceless cytosolic delivery of any protein of interest (POI), we explored the potential of bioreversible esterification in this study. Sequential bioorthogonal esterification and CuAAC reactions were established to provide model POIs, GFP and BSA, with TMU-enabling CAXs attached through bioreversible ester linkages. TMU-tagged POIs were efficiently uptaken into the cytosol of multiple cell lines, most notably into 3D cultured cells, confirming a key advantage of TMU. Despite these successes, we caution that the current approach is not as practically useful as it might appear because the esterification of POIs reduces negative surface charges. With overall anionic proteins, carboxylate removal increases the isoelectric point toward isoelectric precipitation at pH = 7. This conclusion implies that future efforts toward traceless TMU tags for general use should focus on the removal of positive rather than negative charges from protein surfaces to drive anionic proteins away from isoelectric precipitation. Thus, while our results demonstrate that access to traceless TMU tags as such is unproblematic, the construction of generally useful small-molecule TMU tools for the cytosolic

Research Article
doi.org/10.1002/ceur.202300029

delivery of native proteins will be challenging, but also most impactful.

Experimental Section

Please see Supporting Information.

Acknowledgements

We thank B. Lim, X.-X. Chen, T. Kato and the group of J. Waser for contributions to inhibitor synthesis, the NMR, MS, ACCESS and Bioimaging platforms for services, and the University of Geneva, the National Centre of Competence in Research (NCCR) Chemical Biology (51NF40-185898), the NCCR Molecular Systems Engineering (51NF40-205608), as well as the Swiss NSF for financial support (Swiss-ERC Advanced Grant TIMEUP, TMAG-2_209190; Excellence Grant 200020 204175).

Conflict of Interests

The authors declare no conflict of interest.

Data Availability Statement

The data that support the findings of this study are available in the supplementary material of this article.

Keywords: bioconjugation · bioreversible esterification · isoelectric precipitation · protein delivery · spheroids · thiol-mediated uptake · traceless delivery

[1] I. Nakase, H. Akita, K. Kogure, A. Gräslund, Ü. Langel, H. Harashima, S. Futaki, *Acc. Chem. Res.* **2012**, *45*, 1132–1139.
[2] E. G. Stanzl, B. M. Trantow, J. R. Vargas, P. A. Wender, *Acc. Chem. Res.* **2013**, *46*, 2944–2954.
[3] C. Bechara, S. Sagan, *FEBS Lett.* **2013**, *587*, 1693–1702.
[4] H. D. Herce, A. E. Garcia, M. C. Cardoso, *J. Am. Chem. Soc.* **2014**, *136*, 17459–17467.
[5] J. M. Priegue, D. N. Crisan, J. Martínez-Costas, J. R. Granja, F. Fernandez-Trillo, J. Montenegro, *Angew. Chem. Int. Ed.* **2016**, *55*, 7492–7495.
[6] N. Sakai, S. Matile, *J. Am. Chem. Soc.* **2003**, *125*, 14348–14356.
[7] Q. Laurent, R. Martinent, B. Lim, A.-T. Pham, T. Kato, J. López-Andarias, N. Sakai, S. Matile, *JACS Au* **2021**, *1*, 710–728.
[8] S. Du, S. S. Liew, L. Li, S. Q. Yao, *J. Am. Chem. Soc.* **2018**, *140*, 15986–15996.
[9] J. Zhou, Z. Shao, J. Liu, Q. Duan, X. Wang, J. Li, H. Yang, *ACS Appl. Bio Mater.* **2020**, *3*, 2686–2701.
[10] S. Ulrich, *Acc. Chem. Res.* **2019**, *52*, 510–519.
[11] A. G. Torres, M. J. Gait, *Trends Biotechnol.* **2012**, *30*, 185–190.
[12] G. Gasparini, E.-K. Bang, G. Molinard, D. V. Tulumello, S. Ward, S. O. Kelley, A. Roux, N. Sakai, S. Matile, *J. Am. Chem. Soc.* **2014**, *136*, 6069–6074.
[13] G. Gasparini, G. Sargsyan, E.-K. Bang, N. Sakai, S. Matile, *Angew. Chem. Int. Ed.* **2015**, *54*, 7328–7331.
[14] J. Guo, T. Wan, B. Li, Q. Pan, H. Xin, Y. Qiu, Y. Ping, *ACS Cent. Sci.* **2021**, *7*, 990–1000.
[15] J. Zhou, L. Sun, L. Wang, Y. Liu, J. Li, J. Li, J. Li, H. Yang, *Angew. Chem. Int. Ed.* **2019**, *58*, 5236–5240.
[16] A. Kohata, P. K. Hashim, K. Okuro, T. Aida, *J. Am. Chem. Soc.* **2019**, *141*, 2862–2866.
[17] W. Lang, W. Tan, B. Zhou, Y. Zhuang, B. Zhang, L. Jiang, S. Q. Yao, J. Ge, *Chem. Eur. J.* **2023**, *29*, e202204021.
[18] Q. Mou, X. Xue, Y. Ma, M. Banik, V. Garcia, W. Guo, J. Wang, T. Song, L.-Q. Chen, Y. Lu, *Sci. Adv.* **2022**, *8*, eabo0902.
[19] Z. Shu, I. Tanaka, A. Ota, D. Fushihara, N. Abe, S. Kawaguchi, K. Nakamoto, F. Tomoike, S. Tada, Y. Ito, Y. Kimura, H. Abe, *Angew. Chem. Int. Ed.* **2019**, *58*, 6611–6615.
[20] Q. Laurent, R. Martinent, D. Moreau, N. Winssinger, N. Sakai, S. Matile, *Angew. Chem. Int. Ed.* **2021**, *60*, 19102–19106.
[21] S. Aubry, F. Burlina, E. Dupont, D. Delaroche, A. Joliot, S. Lavielle, G. Chassaing, S. Sagan, *FASEB J.* **2009**, *23*, 2956–2967.
[22] X. Meng, T. Li, Y. Zhao, C. Wu, *ACS Chem. Biol.* **2018**, *13*, 3078–3086.
[23] J. Lu, H. Wang, Z. Tian, Y. Hou, H. Lu, *J. Am. Chem. Soc.* **2020**, *142*, 1217–1221.
[24] R. Martinent, S. Tawffik, J. López-Andarias, D. Moreau, Q. Laurent, S. Matile, *Chem. Sci.* **2021**, *12*, 13922–13929.
[25] R. Bej, A. Ghosh, J. Sarkar, B. B. Das, S. Ghosh, *ChemBioChem* **2020**, *21*, 2921–2926.
[26] P. Kanjilal, K. Dutta, S. Thayumanavan, *Angew. Chem. Int. Ed.* **2022**, *61*, e202209227.
[27] P. Knoll, G. Francesco Racaniello, V. Laquintana, F. Veider, A. Saleh, A. Seybold, N. Denora, A. Bernkop-Schnürch, *Int. J. Pharm.* **2023**, *635*, 122753.
[28] M. L. Qualls, J. Lou, D. P. McBee, J. A. Baccile, M. D. Best, *Chem. Eur. J.* **2022**, *28*, e202201164.
[29] A. Yan, X. Chen, J. He, Y. Ge, Q. Liu, D. Men, K. Xu, D. Li, *Angew. Chem. Int. Ed.* **2023**, *62*, e202303973.
[30] I. S. Shchelik, K. Gademann, *ACS Infect. Dis.* **2022**, *8*, 2327–2338.
[31] F. Coelho, S. Saidjalolov, D. Moreau, O. Thorn-Seshold, S. Matile, *JACS Au* **2023**, *3*, 1010–1016.
[32] Y. Cheng, A.-T. Pham, T. Kato, B. Lim, D. Moreau, J. López-Andarias, L. Zong, N. Sakai, S. Matile, *Chem. Sci.* **2021**, *12*, 626–631.
[33] B. Lim, T. Kato, C. Besnard, A. I. Poblador Bahamonde, N. Sakai, S. Matile, *JACS Au* **2022**, *2*, 1105–1114.
[34] T. Kato, B. Lim, Y. Cheng, A.-T. Pham, J. Maynard, D. Moreau, A. I. Poblador-Bahamonde, N. Sakai, S. Matile, *JACS Au* **2022**, *2*, 839–852.
[35] B. Lim, Y. Cheng, T. Kato, A.-T. Pham, E. Le Du, A. K. Mishra, E. Grinhagena, D. Moreau, N. Sakai, J. Waser, S. Matile, *Helv. Chim. Acta* **2021**, *104*, e2100085.
[36] B. Lim, N. Sakai, S. Matile, *Helv. Chim. Acta* **2023**, *106*, e202300020.
[37] D. Abegg, G. Gasparini, D. G. Hoch, A. Shuster, E. Bartolami, S. Matile, A. Adibekian, *J. Am. Chem. Soc.* **2017**, *139*, 231–238.
[38] Y. Zhu, M. Lin, W. Hu, J. Wang, Z.-G. Zhang, K. Zhang, B. Yu, F.-J. Xu, *Angew. Chem. Int. Ed.* **2022**, *61*, e202200535.
[39] J. V. Jun, Y. D. Petri, L. W. Erickson, R. T. Raines, *J. Am. Chem. Soc.* **2023**, *145*, 6615–6621.
[40] K. A. Mix, J. E. Lomax, R. T. Raines, *J. Am. Chem. Soc.* **2017**, *139*, 14396–14398.
[41] V. T. Ressler, K. A. Mix, R. T. Raines, *ACS Chem. Biol.* **2019**, *14*, 599–602.
[42] Y. D. Petri, C. S. Gutierrez, R. T. Raines, *Angew. Chem. Int. Ed.* **2023**, *62*, e202215614.
[43] A. Alouane, R. Labruère, T. Le Saux, F. Schmidt, L. Jullien, *Angew. Chem. Int. Ed.* **2015**, *54*, 7492–7509.
[44] M. He, J. Li, H. Han, C. A. Borges, G. Neiman, J. J. Røise, P. Hadaczek, R. Mendonsa, V. R. Holm, R. C. Wilson, K. Bankiewicz, Y. Zhang, C. M. Sadlowski, K. Healy, L. W. Riley, N. Murthy, *Chem. Sci.* **2020**, *11*, 8973–8980.
[45] E. K. Lei, S. O. Kelley, *J. Am. Chem. Soc.* **2017**, *139*, 9455–9458.
[46] A. L. Baumann, C. P. R. Hackenberger, *Curr. Opin. Chem. Biol.* **2019**, *52*, 39–46.
[47] K. Maier, E. Wagner, *J. Am. Chem. Soc.* **2012**, *134*, 10169–10173.
[48] K. Shiraiwa, R. Cheng, H. Nonaka, T. Tamura, I. Hamachi, *Cell Chem. Biol.* **2020**, *27*, 970–985.
[49] A. Gonzalez-Valero, A. G. Reeves, A. C. S. Page, P. J. Moon, E. Miller, K. Coulonval, S. W. M. Crossley, X. Xie, D. He, P. Z. Musacchio, A. H. Christian, J. M. McKenna, R. A. Lewis, E. Fang, D. Dovala, Y. Lu, L. M. McGregor, M. Schirle, J. A. Tallarico, P. P. Roger, F. D. Toste, C. J. Chang, *J. Am. Chem. Soc.* **2022**, *144*, 22890–22901.
[50] E. Baslé, N. Joubert, M. Pucheault, *Chem. Biol.* **2010**, *17*, 213–227.
[51] T. H. Wright, M. R. J. Vallée, B. G. Davis, *Angew. Chem. Int. Ed.* **2016**, *55*, 5896–5903.
[52] H. H. Dhanjee, A. Saebi, I. Buslov, A. R. Loftis, S. L. Buchwald, B. L. Pentelute, *J. Am. Chem. Soc.* **2020**, *142*, 9124–9129.

Research Article
doi.org/10.1002/ceur.202300029

[53] A. Istrate, M. B. Geeson, C. D. Navo, B. B. Sousa, M. C. Marques, R. J. Taylor, T. Journeaux, S. R. Oehler, M. R. Mortensen, M. J. Deery, A. D. Bond, F. Corzana, G. Jiménez-Osés, G. J. L. Bernardes, *J. Am. Chem. Soc.* **2022**, *144*, 10396–10406.
[54] M. M. Zegota, M. A. Müller, B. Lantzberg, G. Kizilsavas, J. A. S. Coelho, P. Moscariello, M. Martínez-Negro, S. Morsbach, P. M. P. Gois, M. Wagner, D. Y. W. Ng, S. L. Kuan, T. Weil, *J. Am. Chem. Soc.* **2021**, *143*, 17047–17058.
[55] P. M. S. D. Cal, J. B. Vicente, E. Pires, A. V. Coelho, L. F. Veiros, C. Cordeiro, P. M. P. Gois, *J. Am. Chem. Soc.* **2012**, *134*, 10299–10305.
[56] K. Porte, M. Riomet, C. Figliola, D. Audisio, F. Taran, *Chem. Rev.* **2021**, *121*, 6718–6743.
[57] J. López-Andarias, J. Saarbach, D. Moreau, Y. Cheng, E. Derivery, Q. Laurent, M. González-Gaitán, N. Winssinger, N. Sakai, S. Matile, *J. Am. Chem. Soc.* **2020**, *142*, 4784–4792.
[58] N. Declas, J. R. J. Maynard, L. Menin, N. Gasilova, S. Götze, J. L. Sprague, P. Stallforth, S. Matile, J. Waser, *Chem. Sci.* **2022**, *13*, 12808–12817.
[59] K. M. Cheah, J. V. Jun, K. D. Wittrup, R. T. Raines, *Mol. Pharmaceutics* **2022**, *19*, 3869–3876.
[60] A. A. Tokmakov, A. Kurotani, K.-I. Sato, *Front. Mol. Biosci.* **2021**, *8*, 775736.
[61] G. W. Hofland, A. de Rijke, R. Thiering, L. A. M. van der Wielen, G.-J. Witkamp, *J. Chromatogr. B* **2000**, *743*, 357–368.
[62] A. Kurotani, A. A. Tokmakov, K.-I. Sato, V. E. Stefanov, Y. Yamada, T. Sakurai, *BMC Mol. Cell Biol.* **2019**, *20*, 36.
[63] I. Shybeka, J. R. J. Maynard, S. Saidjalolov, D. Moreau, N. Sakai, S. Matile, *Angew. Chem. Int. Ed.* **2022**, *61*, e202213433.
[64] L. Zong, E. Bartolami, D. Abegg, A. Adibekian, N. Sakai, S. Matile, *ACS Cent. Sci.* **2017**, *3*, 449–453.
[65] T. Chen, Y. Han, M. Yang, W. Zhang, N. Li, T. Wan, J. Guo, X. Cao, *Biochem. Biophys. Res. Commun.* **2003**, *303*, 1114–1120.
[66] R. Marwaha, S. B. Arya, D. Jagga, H. Kaur, A. Tuli, M. Sharma, *J. Cell Biol.* **2017**, *216*, 1051–1070.

Version of record online: ■■, ■■

RESEARCH ARTICLE

Bioreversible esterification is assessed as possible strategy to create traceless TMU tags that would ultimately make thiol-mediated uptake accessible for general use in practice. The results highlight the power of TMU to penetrate deep tissue and confirm isoelectric precipitation as central challenge in protein delivery.

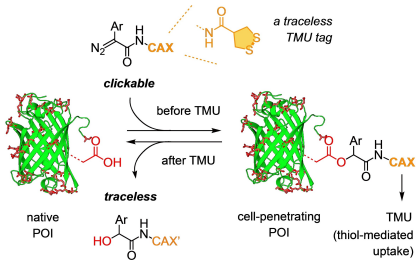

*Dr. J. R. J. Maynard, Dr. S. Saidjalolov, M.-C. Velluz, S. Vossio, Prof. C. Aumeier, Dr. D. Moreau, Dr. N. Sakai, Prof. S. Matile**

1 – 8

Toward a Traceless Tag for the Thiol-Mediated Uptake of Proteins